2019 16th International Conference on Electrical Engineering, Computing Science and Automatic Control (CCE)
Mexico City, Mexico. September 11-13, 2019

Frequency Swept to Optimize Focalization at the *Substantia Nigra* in a Rat Head Model using a Semi-Spherical Ultrasound Transducer

Jorge Alberto Rodríguez Ramírez
Department of Electrical Engineering/Bioelectronics
CINVESTAV-IPN
México City, México.
jorge.rodriguezr@cinvestav.mx

Mario Ibrahín Gutiérrez
CONACYT – Instituto Nacional de Rehabilitación, Subdirección de Investigación Biotecnológica, DIIM,
México City, México.
m.ibrahin.gutierrez@gmail.com

Citlalli Trujillo Romero
National Institute of Rehabilitation, Division of Research in Medical Engineering
México City, México.
cjtrujillo@inr.mx

Arturo Vera Hernández
Department of Electrical Engineering/Bioelectronics
CINVESTAV-IPN
México City, México.
arvera@cinvestav.mx

Daniel Martínez-Fong
Department of Physiology, Biophysics and Neuroscience
CINVESTAV-IPN
México City, México.
dmartine@fisio.cinvestav.mx

Lorenzo Leija Salas
Department of Electrical Engineering/Bioelectronics
CINVESTAV-IPN
México City, México.
lleija@cinvestav.mx

***Abstract* – The use of focused ultrasound in the head has been demonstrated to be advantageous for the disruption of the blood-brain barrier (BBB) in a reversible way. With models using the finite element method, it is possible to made approximations of the physical phenomenon to study separately, and together, the parameters affecting the therapy with the objective of saving time and economical sources during the investigation. In this paper, it presented a geometry of focused ultrasound transducer with a parametric analysis to find an effective configuration that can cross the BBB transcranially with reduced effects at the cranium, and that is able to completely radiate the *substantia nigra*. The results indicate that for a rat head, the frequency to obtain a narrow focus with larger amplitude, enough to cover the *substantia nigra*, was 500 kHz. The penetration depth increases for lower frequencies, but the result is a wider focus that could damage other brain zones.**

Keywords –Finite Element Method, Focused Ultrasound, Blood-Brain Barrier, acoustic field, ultrasound pressure, thermal propagation.

I. Introduction

Ultrasound has been shown to be an advantageous tool in the clinical application for the opening of the blood-brain barrier (BBB) [1]. One of its modalities is the focused ultrasound (FUS), which allows you to create a focus in a specific place at a desired distance. The FUS has been implemented in other areas like in therapy for the management of benign tumors [2], or for surgery of tissue removal for the study of changes in their mechanical properties [3]. FUS has been also proposed to be used to open the BBB safely with the presence of a skull [4] and using craniotomies [5]. However, the main problem is the attenuation of ultrasound by the skull when used transcranially [6].

In the area of ultrasound, different studies has been made about simulation of transducers and tissues, as well as their behavior [7]. The works carried out in the acoustic area include the design of transducers that emit an ultrasonic beam in a localized way to reach a specific desired area like the *substantia nigra* [8]. One point to consider is the damage produced by the thermal effects that occur when the ultrasonic beam is applied in the tissue for a prolonged time [9]. These simulations are supported with experiments on different types of animal models [10]. These jobs often lead to the same purpose by different methods, achieving the opening of the BBB [11],[12].

This paper presents the proposal of a focused ultrasound transducer with characteristics (geometry, diameter, frequency) that permit to achieve an ultrasonic beam capable of crossing the skull of a rat model to position a focus on the *substantia nigra*. The analysis was made with a frequency swept using a fixed geometry for achieving the objective of reaching a specific point without being too invasive, specifically, reaching the *substantia nigra* and avoiding damaging other structures; the heat produced by the ultrasound was also analyzed to verify no-overheating the cranium. The final application of the ultrasound for this very specific region of the brain is beyond the scope of this paper.

II. Methods

A. Theoretical basis

To understand the ultrasound propagation generated for the transducer and the thermal effects produced in the volume, the problem was solved based on the next equations. The stable and harmonic ultrasound propagation can be determined with the acoustic wave equation given by

978-1-7281-4840-3/19/$31.00 ©2019 IEEE

$$\nabla^2 p + k_{eq}^2 p = 0 \quad (1)$$

where p is the total pressure and k_{eq}^2 is the wavenumber When the wavenumber is real, the wave equation is only valid for lineal propagation.

Assuming a harmonic ultrasound generation, the pressure on the radiator surface can be related to its normal acceleration [9] using

$$a_0 = \frac{\omega}{\rho c} p e^{j(\omega t + \frac{\pi}{2})} \quad (2)$$

where a_0 is the normal acceleration, ρ is the density of the material, c is the speed sound of the medium, p is the amplitude of the pressure on the radiator surface. We can determine the pressure on the radiator surface from the acoustic power by using the other equations shown in [9].

The heat propagation can be explained with the Pennes bioheat thermal equation given by

$$\rho C_p \frac{\delta T}{\delta t} + \nabla \cdot (-k \nabla T) = Q \quad (3)$$

where C_p is the heat capacity at constant pressure, k the thermal conductivity, T is the initial temperature, Q is the external heat source. For our case, we can determine Q that is related to the pressure by

$$Q_{ext} = \frac{\alpha p^2}{\rho c} \quad (4)$$

where α is the coefficient of acoustic absorption which was considered the same as attenuation (neglecting scattering).

B. Finite element analysis

For solving the main differential equations presented, the simulation was made with the Finite Element Method (FEM) using COMSOL Multiphysics (COMSOL Inc., Sweden) on a workstation with 64-GB RAM and 3.00-GHz 4-core processor; however, for the problem conditions, less computational resources could be possible. For the FEM solution, it was implemented a 2D axisymmetric geometry that consists of a concave transducer very similar to a helmet that cover great part of the head rat with the purpose to deliver the energy to the cranium more uniformly with low power and reduce heating of the skull of the rat (see Fig. 1). The transducer was made with a radius of 19.5 mm simulating only the front face of the material with the purpose to know the focal depth produced by this and the heating area in the brain tissue and the cortical skull bone.

In Fig. 1, it is also showed every domain of the simulation. Domain 1 is the medium in which the tissue is submerged, in this case is water; the domain 2 is the skull bone of a rat; the domain 3 is the brain. Vertical central boundary is the symmetry axis, and the curved boundary 4 is the radiator boundary, i.e. the transducer, with the determined acceleration of Eq. 2. The rest of the boundaries were set to have the acoustic impedance of water, to reduce wave reflections; thermally, those boundaries were set to 36 °C, which was the temperature of the initial conditions that corresponds to the central temperature of rats.

The simulation was carried out in two parts. The first one was planned to analyze the parameters of a transducer to produce an acceptable focus into the rat head. For this, we proposed a parametric swept of frequencies to find the value that allow us to generate an ultrasound distribution that can cross the rat cranium, using a fixed transducer geometry. This parametric swept starts at a frequency of 500 kHz and finish at 3.5 MHz with steps of 100 kHz. The acoustic pressure distributions were study to determine a transducer configuration that produces an acceptable focus size to cover the *substantia nigra*, with less reverberation between the transducer and the cranium. The second part of the simulation was to determine the heat produced 10 W of power by the transducer configuration found in the first analysis, based on [9]. For this second part, Eq. (3) was solved with the FEM under the conditions already detailed.

The mesh applied in the model was established according to the wavelength (λ) of the materials of the model. The wavelength obtained was divided by 11, which was based on an analysis of convergence by minimizing the error of the solution vs the time required to get that solution [9]. Convergence was verified with smaller meshes having an error of 0.01% between the chosen one and a mesh of 12 elements per wavelength; the time required to solve these problems with 11 and 12 elements per wavelength was about 3.8 min and 6.3 min, respectively, with negligible improvement in the quality of the solution. Then, the final mesh of 11 elements was chosen. In Table 1, the properties used in each domain for the acoustic and heating simulations are presented.

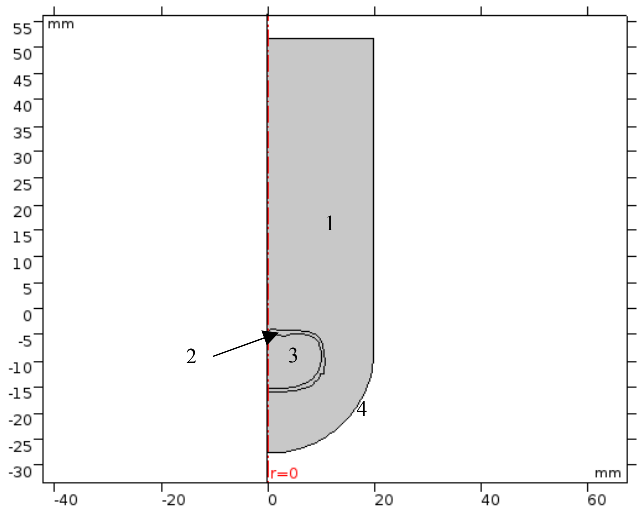

Fig. 1 – Geometry of the simulation. Every domain is different: 1.- Water, 2.- Skull bone, 3.- Brain tissue. Boundary 4 represents the transducer.

TABLE 1.- Acoustic and thermal properties of simulated tissue [13][14]

Domain	Speed of sound (m/s)	Attenuation (Np/m)	Heat capacity (J/(kg·K))	Thermal conductivity (W/(m·K))	Density (kg/m^3)
Water	1500	0	4178	0.60	997
Brain	1546	6	3696	0.49	911
Skull bone	2814	180	1313	0.32	1908

III. RESULTS AND DISCUSSION

The results present both the acoustic propagation and the heat produced at the best-case scenario of the acoustic propagation analyzed. It was obtained different propagation maps that demonstrate the focused pressure inside the brain. It was required, as the optimal result, the production of a focus with the enough size to cover the *substantia nigra* of a murine model, which should pass through the skull with a little thermal damage. The ideal result should be a focus with no increase of temperature, but the actual results should be close enough to not provoke damages of other brain tissues.

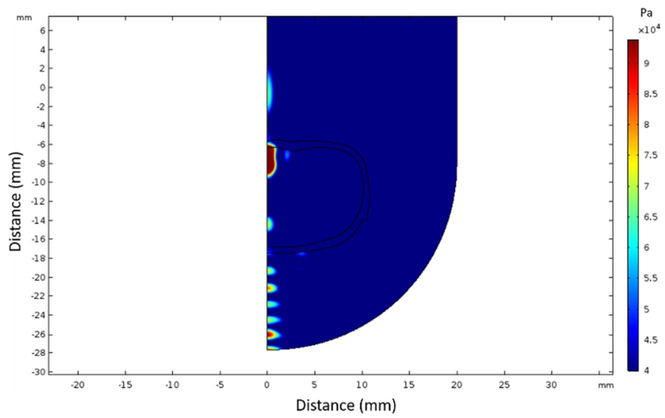

Fig. 2 – Focused pressured map at 500 kHz.

Figure 2 shows the focus generated at 500 kHz. In the pressure distribution it can be seen a focus with a large intensity at 20 mm approximately from the center of the transducer. The other pressure peaks into the head shown in the figure should be considered important, since they are produced by other means of focusing, for instance, by the cranium. However, the pressure levels generated in them are reduced compared with the focus. The peaks between the head and the transducer are produced by the reverberations of the ultrasound after the signal is continuously reflected by the cranium. However, because the water has a negligible absorption, those peaks do not produce any heating effect. If the medium which the ultrasonic beam propagates were different, more losses would be produced before the energy arrive to the target zone, which then would provoke the generated focus being even smaller.

To compare results using different frequencies, the pressure on the propagation axis was plot in Fig. 3 for three different cases, all having the same amplitude of acceleration. The frequency values showed in Fig. 3 are 500 kHz (black line), 2 MHz (blue line) and 3.5 MHz (red line). From these graphs, we can see that the focus is narrower when the frequency increases, but also the pressure at the focus changes; that is, the area of the focus starts to be larger, so, it begins to differ from our main objective. This could occur because of bone reflections that produce reverberations inside the cranium, increasing hotspots outside the focus. Therefore, even if the graph shows that increasing the frequency will also increase the pressure level, the result using higher frequencies would not be optimal since those do not cover the entire *substantia nigra*.

When the frequency is 2 MHz (shown in Fig. 4), the area of distribution is narrower with respect to lower frequencies; this means the focus is small and the size would not be enough to cover the *substantia nigra*. However, the pressure amplitude at the focus increase as expected, because the concentration of the energy in a smaller region. However, this was not true for 3.5 MHz. As seen in Fig. 3, for a frequency of 3.5 MHz, the pressure amplitude is smaller than the others, and the pressure distribution at the focus is narrower. This occurs because when the frequency grows, it is more difficult to cross the skull due to the difference of acoustic impedances and the high attenuation of the ultrasonic beam that it produces [6]. Selecting a good frequency is important for our investigation because it will be used to obtain a custom-made transducer for the experimental work. The generated focus is adequate for our purposes in both location (depth) and size.

The heat distribution was determined for the more optimal result obtained in the previous step, which was the simulation using 500 kHz ultrasound radiation. Figure 5 shows the contour plot of the temperature generated in the simulated rat brain. It can be seen how the highest heating rate occurs at the focus produced by the transducer; however, the heating is also given, although to a lesser extent, in the skull, where the ultrasonic beam hits. This effect not produced in other parts of the cranium could be because the rat cranium is flat in the upper part of the head, which produced additive ultrasound reverberations between the cranium and the transducer, which increase the temperature at that region. However, the final temperature in the cranium was not importantly large compared with the temperature at the focus. We can consider that this transducer geometry effectively helped in decreasing the damage on the cranium by increasing the radiating area of the head.

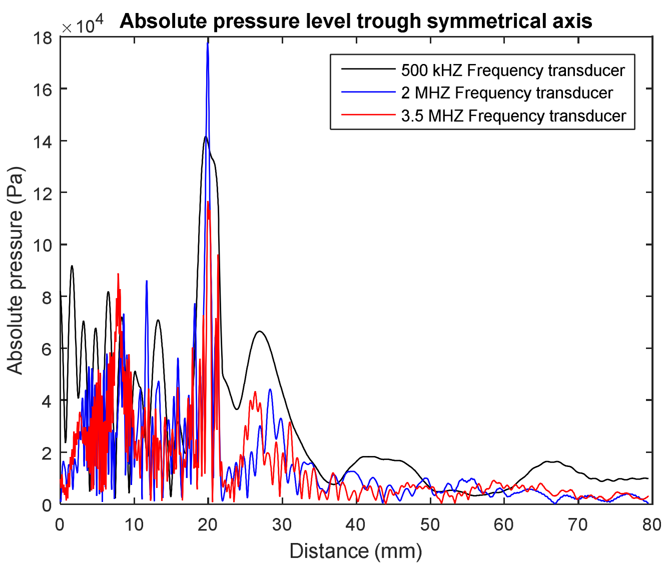

Fig. 3 – Pressure distribution along the symmetric axis of the model. It was made a parametric swept to obtain these results. The black line represents the result of 500 kHz, the blue line is the 2 MHz and the red line is the 3.5 MHz.

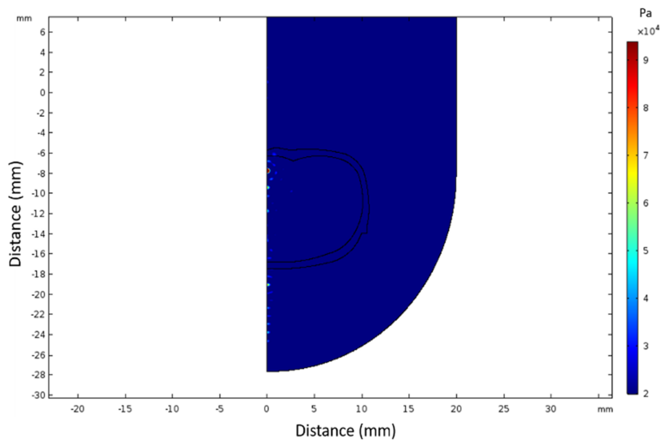

Fig. 4– Focused pressured map at 2 MHz.

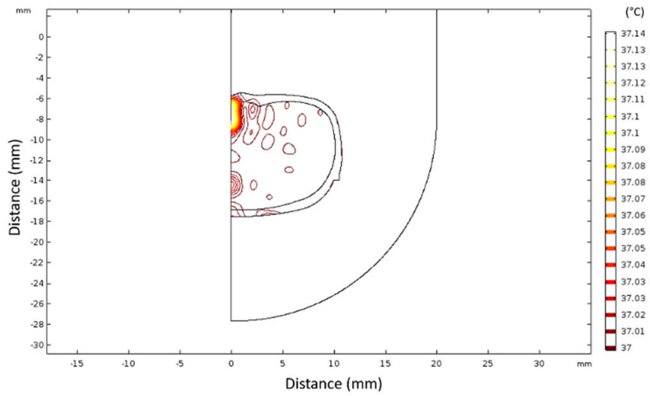

Fig. 5 – Contour temperature distribution in the brain.

IV. Conclusions

This paper was made with the purpose of determining an adequate focused pressure distribution across the head of a model rat that can cover the *substantia nigra*. The heat distribution is related to the pressure generated by the ultrasound. With this simulation, it was also determined that the frequency of the ultrasound in a transducer affects the transmission through the cortical bone of a rat head; from this, we concluded that transmission is higher for low frequencies, but the focus is larger and wider.

For the best-case scenario obtained in this paper, it has been found an acceptable combination of transducer parameters that can produce a temperature increase at the focus, with reduced temperature increase at the skull, having the adequate size to effectively cover the *substantia nigra*.

Acknowledgment

We appreciate the funding for the development of the work presented project: ERAnet-EMHE 200022, CYTED-DITECROD-218RT0545, CB2015-257966, and Proyecto IV-8 call Amexcid-Auci 2018-2020.

References

[1] G. Samiotaki, F. Vlachos, Y. S. Tung, and E. E. Konofagou, “Permeability and reversibility timeline study of the focused-ultrasound induced blood-brain barrier opening at distinct pressures and microbubble sizes in vivo,” in *IEEE International Ultrasonics Symposium, IUS*, 2011.

[2] V. Y. T. Cheung, “High-intensity focused ultrasound therapy,” *Best Pract. Res. Clin. Obstet. Gynaecol.*, vol. 46, pp. 74–83, 2018.

[3] C. Maleke and E. E. Konofagou, “In vivo feasibility of real-time monitoring of focused ultrasound surgery (FUS) using harmonic motion imaging (HMI),” *IEEE Trans. Biomed. Eng.*, vol. 57, no. 1, pp. 7–11, 2010.

[4] J. J. Choi, M. Pernot, S. A. Small, and E. E. Konofagou, “Noninvasive, transcranial and localized opening of the blood-brain barrier using focused ultrasound in mice,” *Ultrasound Med. Biol.*, vol. 33, no. 1, pp. 95–104, 2007.

[5] D. A. Hernandez, M. I. Gutierrez, A. Vera, D. Martinez-Fong, and L. Leija, “Simulation and in vivo validation of craniotomies in rats for the disruption of the blood brain barrier with focused ultrasound for drug delivery,” in *2017 14th International Conference on Electrical Engineering, Computing Science and Automatic Control, CCE 2017*, 2017, pp. 1–5.

[6] G. Pinton, J. F. Aubry, E. Bossy, M. Muller, M. Pernot, and M. Tanter, “Attenuation, scattering, and absorption of ultrasound in the skull bone,” *Med. Phys.*, vol. 39, no. 1, pp. 299–307, 2012.

[7] W. Larbi and J. F. Deü, “Reduced order finite element formulations for vibration reduction using piezoelectric shunt damping,” *Appl. Acoust.*, vol. 147, no. March, pp. 111–120, 2019.

[8] D. A. Hernández, M. I. Gutiérrez, A. Vera, and L. Leija, “Simulation and in vivo Validation of Craniotomies in Rats for the Disruption of the Blood Brain Barrier with Focused Ultrasound for Drug Delivery,” pp. 2–6, 2017.

[9] M. I. Gutierrez, S. A. Lopez-Haro, A. Vera, and L. Leija, “Experimental Verification of Modeled Thermal Distribution Produced by a Piston Source in Physiotherapy Ultrasound,” *Biomed Res. Int.*, vol. 2016, pp. 1–16, 2016.

[10] N. Vykhodtseva, N. McDannold, and K. Hynynen, “Progress and problems in the application of focused ultrasound for blood-brain barrier disruption,” *Ultrasonics*. 2008.

[11] K. F. Bing, G. P. Howles, Y. Qi, M. L. Palmeri, and K. R. Nightingale, “Blood-Brain Barrier (BBB) Disruption Using a Diagnostic Ultrasound Scanner and Definity® in Mice,” *Ultrasound Med. Biol.*, 2009.

[12] Y. Lin *et al.*, “Effect of acoustic parameters on the cavitation behavior of SonoVue microbubbles induced by pulsed ultrasound,” *Ultrason. Sonochem.*, vol. 35, pp. 176–184, 2017.

[13] K. Giering;, O. Minet;, I. Lamprecht;, and G. Muller, “Review of thermal properties of biological tissues,” *SPIE Opt. Eng. Press*, vol. 044, no. August 2018, pp. 45–65, 1995.

[14] A. Feldmann, P. Wili, G. Maquer, and P. Zysset, “The thermal conductivity of cortical and cancellous bone,” *Eur. Cells Mater.*, vol. 35, no. 2000, pp. 25–33, 2018.